ATR acts stage specifically to regulate multiple aspects of mammalian meiotic silencing

Hélène Royo,[1] Haydn Prosser,[2] Yaroslava Ruzankina,[3] Shantha K. Mahadevaiah,[1] Jeffrey M. Cloutier,[1] Marek Baumann,[4] Tomoyuki Fukuda,[5] Christer Höög,[5] Attila Tóth,[4] Dirk G. de Rooij,[6] Allan Bradley,[2] Eric J. Brown,[3] and James M.A. Turner[1,7]

[1]Division of Stem Cell Biology and Developmental Genetics, Medical Research Council, National Institute for Medical Research, London NW7 1AA, United Kingdom; [2]The Wellcome Trust Sanger Institute, Hinxton, Cambridge CB10 1SA, United Kingdom; [3]Abramson Family Cancer Research Institute, Department of Cancer Biology, University of Pennsylvania School of Medicine, Philadelphia, Pennsylvania 19104, USA; [4]Institute of Physiological Chemistry, Technische Universität Dresden, Dresden 01307, Germany; [5]Department of Cell and Molecular Biology, Karolinska Institutet, Stockholm SE-171 77, Sweden; [6]Center for Reproductive Medicine, Academic Medical Center, University of Amsterdam, Amsterdam 1105 AZ, The Netherlands

In mammals, homologs that fail to synapse during meiosis are transcriptionally inactivated. This process, meiotic silencing, drives inactivation of the heterologous XY bivalent in male germ cells (meiotic sex chromosome inactivation [MSCI]) and is thought to act as a meiotic surveillance mechanism. The checkpoint protein ATM and Rad3-related (ATR) localizes to unsynapsed chromosomes, but its role in the initiation and maintenance of meiotic silencing is unknown. Here we show that ATR has multiple roles in silencing. ATR first regulates HORMA (Hop1, Rev7, and Mad2) domain protein HORMAD1/2 phosphorylation and localization of breast cancer I (BRCA1) and ATR cofactors ATR-interacting peptide (ATRIP)/topoisomerase 2-binding protein 1 (TOPBP1) at unsynapsed axes. Later, it acts as an adaptor, transducing signaling at unsynapsed axes into surrounding chromatin in a manner that requires interdependence with mediator of DNA damage checkpoint 1 (MDC1) and H2AFX. Finally, ATR catalyzes histone H2AFX phosphorylation, the epigenetic event leading to gene inactivation. Using a novel genetic strategy in which MSCI is used to silence a chosen gene in pachytene, we show that ATR depletion does not disrupt the maintenance of silencing and that silencing comprises two phases: The first is dynamic and reversible, and the second is stable and irreversible. Our work identifies a role for ATR in the epigenetic regulation of gene expression and presents a new technique for ablating gene function in the germline.

[*Keywords*: ATR; meiosis; sex chromosomes]

Supplemental material is available for this article.

Received April 9, 2013; revised version accepted May 31, 2013.

During mammalian meiosis, homologous chromosomes synapse and recombine, generating crossovers that are essential for correct chromosome segregation (Handel and Schimenti 2010). In order to prevent the generation of aneuploid gametes, meiotic cells exhibiting defects in synapsis or recombination are eliminated from the germ cell pool by meiotic surveillance mechanisms (Nagaoka et al. 2012). The molecular pathways that constitute these surveillance mechanisms are currently not well understood.

One proposed mechanism by which unsynapsed chromosomes trigger germ cell arrest is meiotic silencing (Baarends et al. 2005; Turner et al. 2005; Ichijima et al. 2012). At the onset of pachytene, genes located on unsynapsed chromosomes are inactivated, remaining so for the rest of meiosis and, in the male, after this time (Greaves et al. 2006; Namekawa et al. 2006; Turner et al. 2006). Meiotic silencing has been proposed to cause arrest by starving germ cells of essential gene products (Burgoyne et al. 2009). Other suggested functions include silencing of transposable elements and inhibition of transcription at sites of meiotic DNA double-strand break (DSB) formation (Inagaki et al. 2010). During wild-type male meiosis, the heterologous X and Y (sex) chromosomes remain largely unsynapsed, and this triggers meiotic silencing of X- and Y-linked genes. The resulting phenomenon, known as meiotic sex chromosome inactivation (MSCI) (McKee and Handel 1993; Yan and McCarrey 2009), affects protein-coding but not microRNA genes (Song et al. 2009) and results in the formation of the heterochromatic sex body (Solari 1974). MSCI is essential for male fertility (Royo et al. 2010) and represents an ideal paradigm for studying the epigenetics of meiotic silencing.

[7]**Corresponding author**
E-mail jturner@nimr.mrc.ac.uk
Article is online at http://www.genesdev.org/cgi/doi/10.1101/gad.219477.113.

Meiotic silencing involves two sets of proteins: "sensors," which localize to axial elements (AEs) and sense asynapsis, and "effectors," which localize to the chromatin loops associated with unsynapsed AEs, causing gene silencing over a considerable distance. The AE component synaptonemal complex protein 3 (SYCP3) (Kouznetsova et al. 2009), HORMA (Hop1, Rev7, and Mad2) domain proteins HORMAD1 (Daniel et al. 2011) and HORMAD2 (Wojtasz et al. 2012), and breast cancer I gene BRCA1 (Turner et al. 2004) have been identified as sensors: BRCA1 accumulates along unsynapsed AEs in an SYCP3-, HORMAD1-, and HORMAD2-dependent manner, and mice deficient in any of these four proteins exhibit MSCI defects. In contrast, the mediator of DNA damage checkpoint 1 (MDC1) (Ichijima et al. 2011) and histone variant H2AFX (Fernandez-Capetillo et al. 2003) are silencing effectors: In *MDC1*- and *H2AFX*-nulls, gene silencing within the chromosome loops does not occur. Ser139 phosphorylation of H2AFX (γH2AFX) is the key epigenetic event triggering MSCI, with spreading of this modification along chromosome loops being MDC1-dependent (Ichijima et al. 2011). *Ago4*$^{-/-}$ mice also exhibit a defect in MSCI, associated with defective γH2AFX localization on the XY bivalent and altered small RNA profiles (Modzelewski et al. 2012).

H2AFX Ser139 phosphorylation is catalyzed by the PI3K-like kinases ataxia telangiectasia mutated (ATM), ATM and Rad3-related (ATR), and DNA-dependent protein kinase (DNA-PK) (Sedelnikova et al. 2003). Which kinase generates γH2AFX on unsynapsed meiotic chromosomes is unclear. H2AFX phosphorylation is preserved on the XY bivalent in *DNA-PK* and *Atm* single nulls (Bellani et al. 2005). This implies that either ATR is the responsible kinase or the PI3K-like kinases act redundantly in this context in a manner already documented in mitotic cells (Stiff et al. 2004). Indeed, both ATR (Turner et al. 2004) and Ser1981-phosphorylated ATM (Hamer et al. 2004) have been found to localize to the XY bivalent during pachytene. Attempts to discriminate between these possibilities have been hampered by the fact that *Atr* ablation causes embryonic lethality (Brown and Baltimore 2000).

A number of other questions concerning the mechanisms underlying meiotic silencing remain unresolved. First, it is unclear how sensing of asynapsis at AEs is transduced into gene silencing along associated chromatin loops. Interestingly, ATR exhibits the unusual property of localizing to both the unsynapsed AEs and the surrounding chromatin of the XY bivalent at the onset of MSCI (Turner et al. 2004). This raises the possibility that it connects the sensing and effector steps in the silencing pathway. Furthermore, the interrelationships between ATR and other silencing factors—e.g., HORMAD1, HORMAD2, BRCA1, MDC1, and H2AFX—have not been examined. In mitotic cells, ATR is recruited to sites of RPA-coated ssDNA through its binding partner, ATR-interacting peptide (ATRIP), with ATR subsequently being activated by DNA topoisomerase 2-binding protein 1 (TOPBP1) (Burrows and Elledge 2008). ATRIP and TOPBP1 localize to the sex chromosomes in male meiosis (Refolio et al. 2011), but how they are recruited there is unclear. Finally, ATR localizes to the XY bivalent from early pachytene until late diplotene; i.e., for some 8–9 d after the initiation of MSCI (Turner et al. 2004). This raises the questions of whether meiotic silencing is a dynamic process, involving continuous H2AFX phosphorylation, and whether ATR is required for the maintenance of the inactive state.

To interrogate these points, we generated two forms of conditional *Atr* mutant mice. The first uses a Cre-recombinase-driven approach to delete ATR at the initiation of silencing, and the second implements a novel, MSCI-driven silencing strategy to deplete ATR levels at later stages, after silencing has been established.

Results

ATR ablation causes meiotic arrest and defective H2AFX phosphorylation

To examine the role of *Atr* in MSCI, we used a previously described tamoxifen-inducible Cre-ERT2 approach in which *Cre-ERT2* expression is driven from the human ubiquitin C promoter (Ruzankina et al. 2007). *Atr*$^{flox/-}$ males treated with tamoxifen and killed 3 mo later exhibit spermatogonial stem cell loss and no germ cells in the seminiferous epithelium (Ruzankina et al. 2007). We therefore used a modified strategy in which *Atr*$^{flox/-}$ males and *Atr*$^{flox/+}$ controls received 1 wk of tamoxifen treatment and were then killed at earlier time points after treatment cessation (see the Materials and Methods for further details on treatment strategy). Here we focus only on the meiotic silencing phenotypes.

Beginning at 3 d after cessation of tamoxifen treatment, we observed abnormal nuclear morphology in spermatocytes from *Atr*$^{flox/-}$ males, extending from stages I to VI of the seminiferous cycle, as assayed by testis histology (Fig. 1A). This was associated with meiotic germ cell loss between stages III and V, corresponding to mid-pachytene. The level of ATR protein, determined by Western blotting (Fig. 1B) and immunostaining of testis sections (Fig. 1C), was globally reduced in *Atr*$^{flox/-}$ testes 3-d after treatment cessation relative to *Atr*$^{flox/+}$ controls. This time point was therefore chosen for further characterization of the *Atr*-null phenotype.

To assess the degree of ATR depletion in *Atr*$^{flox/-}$ testes in greater detail, we performed immunostaining on surface spreads in combination with an antibody to the AE marker SYCP3. In *Atr*$^{flox/+}$ control males, we first observed ATR staining at zygotene, where it appeared as foci on AEs (Fig. 1D). Later, at pachytene, ATR was observed exclusively on the AEs and the chromatin of the XY bivalent (Fig. 1D). In *Atr*$^{flox/-}$ males, the ATR staining patterns at zygotene and pachytene were lost (Fig. 1D); in the latter cell type, traces of ATR were observed at the pseudoautosomal region (PAR) (Fig. 1D, and see the figure legends for number of cells examined for this and later experiments). Normal ATR staining was observed in *Atr*$^{flox/-}$ late pachytene and diplotene cells due to the fact that these more advanced cell types had not undergone *Atr* deletion (Fig. 1D; see below for further discussion).

ATM is required for H2AFX phosphorylation at DNA DSBs during leptotene, while ATR has been proposed to

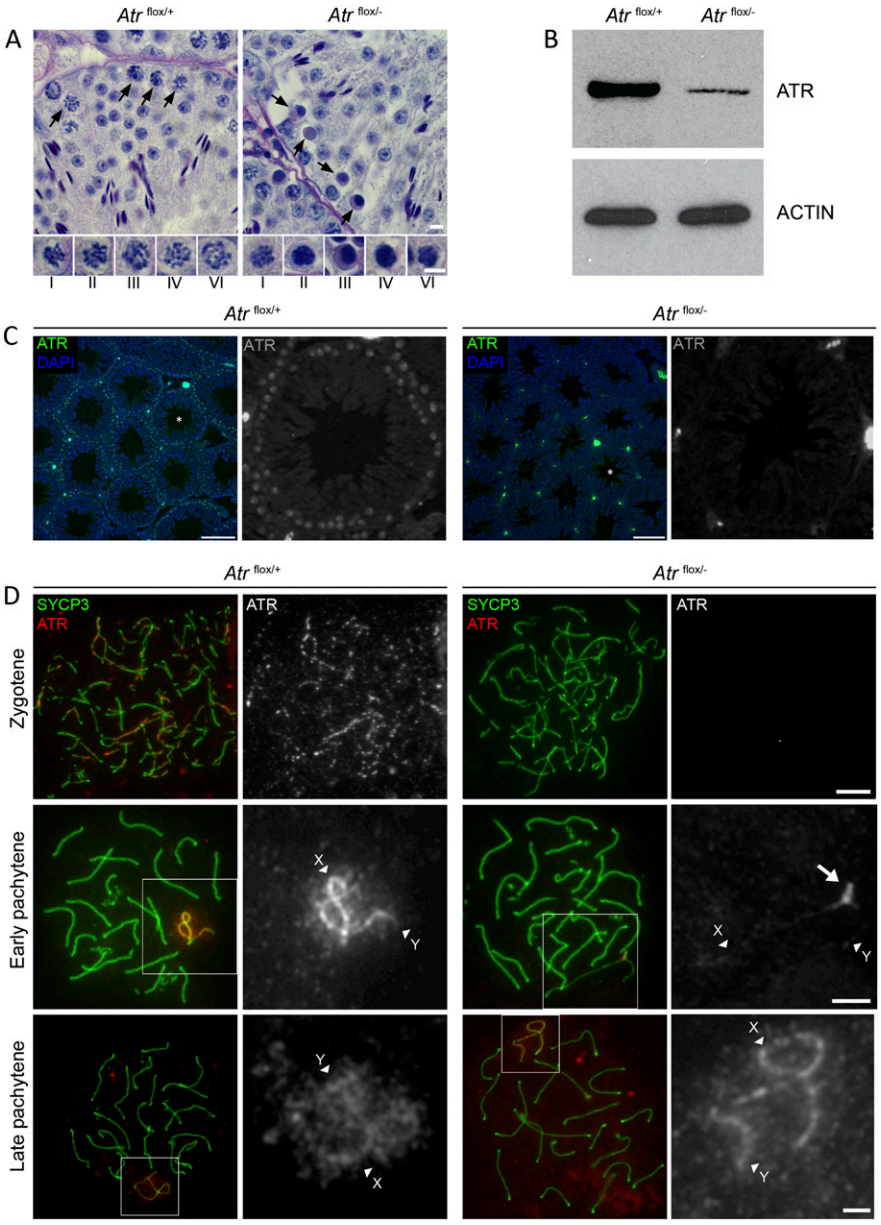

Figure 1. ATR ablation in $Atr^{flox/-}$ mice causes pachytene spermatocyte losses. (*A*) PAS-stained stage IV tubule sections from $Atr^{flox/+}$ and $Atr^{flox/-}$ mice showing pachytene germ cell death in $Atr^{flox/-}$ males. Arrows point to healthy ($Atr^{flox/+}$ panel) versus dying ($Atr^{flox/-}$ panel) pachytene cells. Note that post-meiotic cells are present in the $Atr^{flox/-}$ section because of the transient nature of the Cre-ERT2-mediated knockdown. (*Bottom*) Pachytene spermatocytes at stages I–IV and VI. Abnormal morphology is visible from stages I to VI, but a major wave of cell death happens at stages III and IV. Bars, 5 μm. (*B*) Western blot showing reduction of ATR protein level in $Atr^{flox/-}$ testis compared with $Atr^{flox/+}$. β-ACTIN is used as a loading control. (*C*) Immunofluorescence for ATR on control and $Atr^{flox/-}$ testis sections at low magnification (color), with tubules marked with an asterisk also shown under high magnification (black and white). In control spermatocytes, ATR is present as a diffuse signal in the nucleoplasm and as a bright signal in the sex body. These signals are dramatically reduced in $Atr^{flox/-}$ sections. Bar, 100 μm. (*D*) Surface spread images of $Atr^{flox/-}$ and control spermatocytes showing substantial depletion of ATR at zygotene (*top* row; n = 50 nuclei) and early pachytene (*middle* row; n = 100 nuclei) in $Atr^{flox/-}$ males. Residual ATR can be seen at the PAR of $Atr^{flox/-}$ spermatocytes (arrow). (*Bottom* row) Those late pachytene cells that have survived mid-pachytene cell death retain ATR staining (n = 100 nuclei). X and Y AEs are indicated by arrowheads. Bar, 5μm.

regulate H2AFX phosphorylation at DNA DSBs during zygotene (Bellani et al. 2005; Turner et al. 2005). ATR and Ser1981-phosphorylated ATM have both been localized to the XY chromatin at early pachytene (Hamer et al. 2004; Turner et al. 2004), and it is therefore unclear what the relative contributions of these kinases are to MSCI-related H2AFX phosphorylation. We observed normal γH2AFX staining patterns during leptotene in $Atr^{flox/-}$ males, but H2AFX phosphorylation at zygotene was dramatically reduced, consistent with ATR being the principle H2AFX kinase at this latter time point (Fig. 2A). In early pachytene $Atr^{flox/-}$ spermatocytes, H2AFX phosphorylation on the unsynapsed regions of the XY chromatin was also attenuated, and γH2AFX was observed only at the PAR (Fig. 2B), presumably due to the presence of residual ATR at this site (Fig. 1D). We subsequently found that the Ser1981-phosphorylated ATM antibody previously shown to exhibit XY chromatin staining (Hamer et al. 2004) gave the same localization pattern in $Atm^{-/-}$ mice (Supplemental Fig. 1A). Thus, although this antibody gives irradiation-dependent staining in spermatogonia and Sertoli cells (Hamer et al. 2004), the XY-staining pattern is nonspecific. We observed no localization of ATM to the XY chromatin or the PAR in either $Atr^{flox/+}$ or $Atr^{flox/-}$ males using two additional ATM antibodies (Supplemental Fig. 1B,C). We conclude that ATR is required for the bulk of H2AFX phosphorylation during zygotene and early pachytene.

H2AFX phosphorylation at early pachytene results in meiotic silencing, which can be assayed by RNA FISH. To examine the role of ATR in silencing, we studied expression of the X-linked gene *Scml2* in $Atr^{flox/-}$ male pachytene cells. *Scml2* is silenced by MSCI, and mice defective in

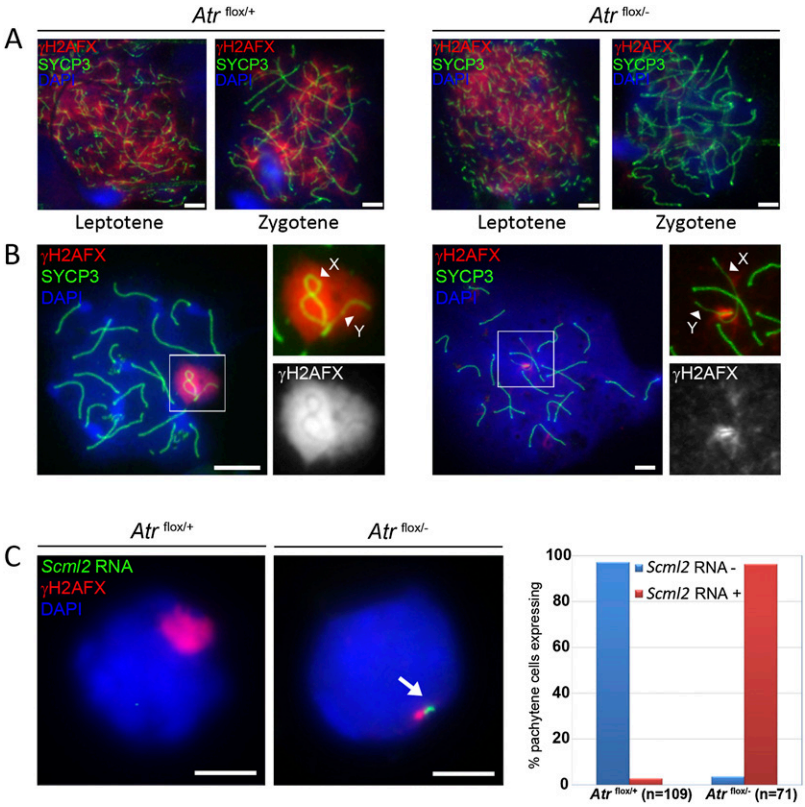

Figure 2. ATR is required for H2AFX phosphorylation at zygotene and pachytene and for meiotic silencing. (*A*) γH2AFX immunofluorescence of $Atr^{flox/+}$ and $Atr^{flox/-}$ spermatocytes showing normal γH2AFX patterns at leptotene (n = 50 nuclei) and loss of γH2AFX staining at zygotene (n = 50 nuclei) in $Atr^{flox/-}$ males. (*B*) Surface spread image of $Atr^{flox/+}$ and $Atr^{flox/-}$ pachytene spermatocytes showing loss of γH2AFX staining at the XY bivalent in $Atr^{flox/-}$ spermatocytes, with γH2AFX observed only at the PAR. Arrowheads point to the X and Y AEs. (*C*) RNA FISH images for $Atr^{flox/+}$ (n = 100 nuclei) and $Atr^{flox/-}$ (n = 100 nuclei) early pachytene cells showing *Scml2* misexpression in $Atr^{flox/-}$ spermatocytes. The RNA FISH signal (arrow) is found close to the γH2AFX-stained PAR. The graph shows the proportion of spermatocytes exhibiting *Scml2* RNA FISH signals in each genotype. Bar, 5 μm.

MSCI show inappropriate *Scml2* expression at early pachytene (Wojtasz et al. 2012). We observed *Scml2* expression in 97% of $Atr^{flox/-}$ early pachytene cells, easily identifiable by their characteristic PAR γH2AFX staining (Fig. 2C). Thus, ATR is essential for the initiation of meiotic silencing.

ATR also regulates localization of silencing factors at unsynapsed AEs

HORMAD1, HORMAD2, and BRCA1 are essential for ATR localization to unsynapsed AEs (Turner et al. 2004; Daniel et al. 2011; Wojtasz et al. 2012). Nevertheless, since the PI3K-like kinases are required for accumulation of various repair proteins at DNA DSBs in mitotic cells, we questioned whether ATR could also reciprocally regulate HORMAD1, HORMAD2, and BRCA1 localization and, as such, function in the sensing step of meiotic silencing.

We observed grossly normal HORMAD1 and HORMAD2 localization to the XY AEs in $Atr^{flox/-}$ males (Fig. 3A), which was confirmed quantitatively (Supplemental Fig. 1D). Interestingly, however, BRCA1 localization at the XY AEs was disrupted (Fig. 3A). Consistent with a role for ATR in regulating BRCA1 localization, we observed ectopic BRCA1 accumulation at the PAR in $Atr^{flox/-}$ males (Fig. 3A). We conclude that BRCA1 and ATR are interdependent in the meiotic silencing pathway.

Hop1, the yeast HORMAD1/2 ortholog, is a known phosphotarget of Mec1, the yeast ATR ortholog (Carballo et al. 2008). It has therefore been proposed that ATR phosphorylates HORMAD1/2 and that this may be essential in mediating certain HORMAD1/2 functions, including meiotic silencing (Fukuda et al. 2012). Indeed, a recent study has shown that HORMAD1 and HORMAD2 are phosphorylated, with Ser375-phosphorylated HORMAD1 (pHORMAD1^{Ser375}) being enriched at unsynapsed AEs (Fukuda et al. 2012). We confirmed localization of pHORMAD1^{Ser375} to the unsynapsed XY AEs (Fig. 3B) and, using a newly synthesized antibody, found that Ser271-phosphorylated HORMAD2 (pHORMAD2^{Ser271}) is also enriched at these sites (Fig. 3B). To test whether these SQ motif HORMAD1 and HORMAD2 modifications were ATR-dependent, we analyzed their localization in $Atr^{flox/-}$ males. Both phospho-epitopes were barely detectable on the XY AEs in $Atr^{flox/-}$ pachytene cells (Fig. 3B). Consistent with ATR being the principal HORMAD1^{Ser375}/HORMAD2^{Ser271} kinase, we observed normal localization of both modified forms to the XY AEs in $Atm^{-/-}$ cells (Fig. 3B).

Next, we wished to investigate the relationship between localization of ATR and that of its cofactors, ATRIP and TOPBP1, to unsynapsed AEs. Interestingly, enrichment of both ATRIP and TOPBP1 to the XY AEs was disrupted in $Atr^{flox/-}$ males, and both proteins accumulated instead at the PAR (Fig. 3C). We conclude that, in addition to its role in H2AFX phosphorylation, ATR regulates the localization of multiple silencing factors at unsynapsed axes.

A positive feedback loop between ATR, MDC1, and H2AFX amplifies the silencing response

In mitotic cells, ATM, MDC1, and H2AFX participate in a positive feedback loop in which MDC1 binds phosphor-

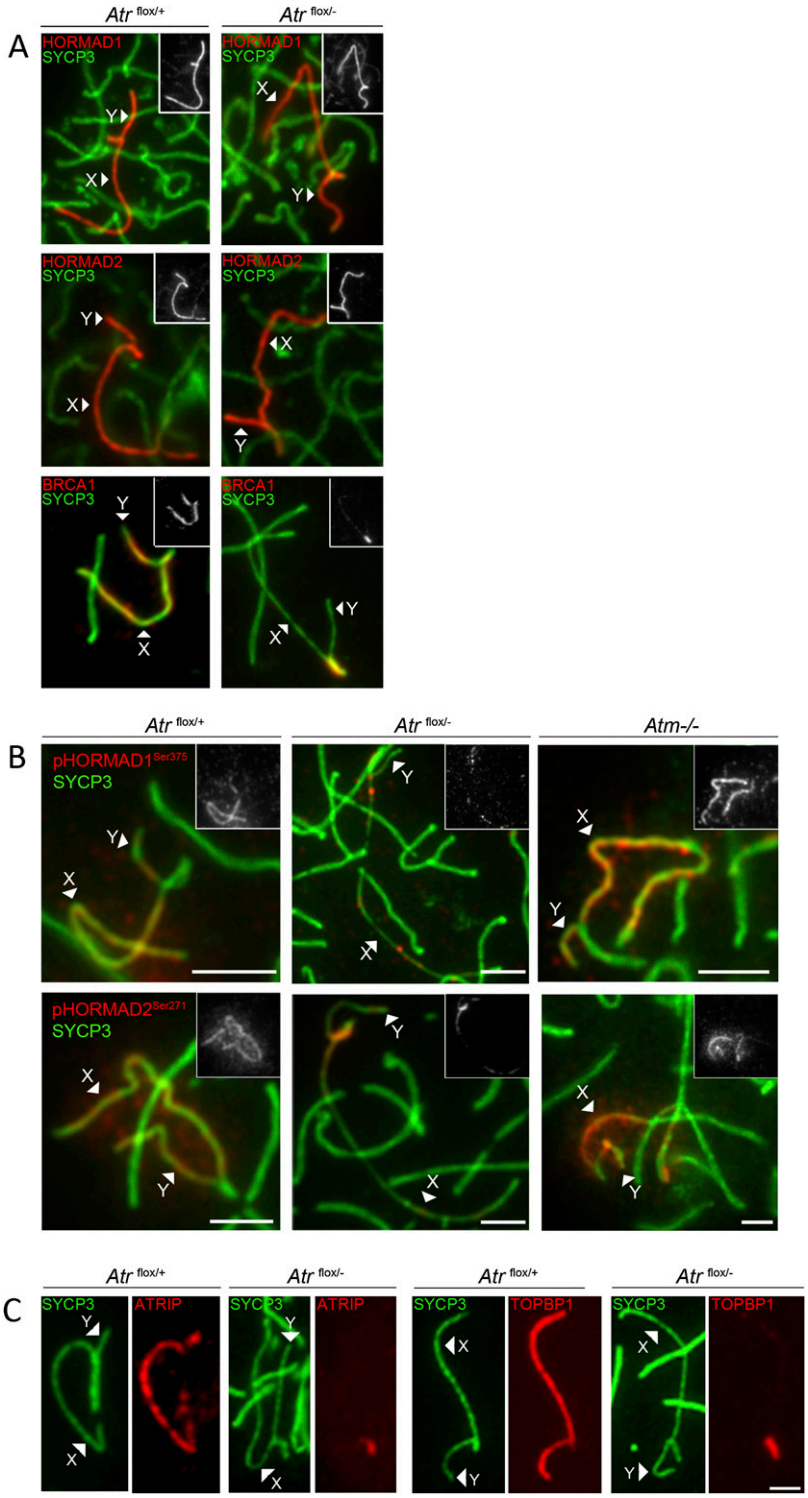

Figure 3. ATR regulates silencing factor localization to unsynapsed axes. (*A*) XY AEs from $Atr^{flox/+}$ and $Atr^{flox/-}$ surface spread pachytene spermatocytes showing normal HORMAD1 (*top* row; $n = 50$ nuclei) and HORMAD2 (*middle* row; $n = 50$ nuclei) and defective BRCA1 (*bottom* row; $n = 50$ nuclei) localization in $Atr^{flox/-}$ males. In $Atr^{flox/-}$ pachytene cells, BRCA1 accumulates at the PAR. The *insets* show HORMAD1, HORMAD2, and BRCA1 staining only. (*B*) XY AEs from $Atr^{flox/+}$ and $Atr^{flox/-}$ surface spread pachytene spermatocytes showing disrupted $HORMAD1^{Ser375}$ (*top* row; $n = 50$ nuclei) and $HORMAD2^{Ser271}$ (*bottom* row; $n = 50$ nuclei) localization in $Atr^{flox/-}$ males. In $Atm^{-/-}$ spermatocytes, $HORMAD1^{Ser375}$ ($n = 50$ nuclei) and $HORMAD2^{Ser271}$ ($n = 50$ nuclei) localization are grossly normal. The *insets* show $HORMAD1^{Ser375}$ and $HORMAD2^{Ser271}$ only. (*C*) XY AEs from $Atr^{flox/+}$ and $Atr^{flox/-}$ surface spread pachytene spermatocytes showing disrupted ATRIP ($n = 50$ nuclei) and TOPBP1 ($n = 50$ nuclei) localization in $Atr^{flox/-}$ males. Both proteins accumulate at the PAR. Arrowheads point to the X and Y AEs. Bar, 5 μm.

ylated H2AFX and subsequently recruits ATM, which catalyzes further H2AFX phosphorylation, thereby amplifying the DNA damage response (Lou et al. 2006). A recent study has found that in the absence of MDC1, spreading of ATR and γH2AFX into the chromatin of unsynapsed AEs is defective, suggesting that an analogous feedback system operates during meiotic silencing (Ichijima et al. 2011). Under this model, the loss of ATR, MDC1, or γH2AFX should affect the localization of the other two silencing factors.

To test this prediction, we analyzed MDC1 immunostaining in $Atr^{flox/-}$ males. MDC1 is a silencing effector and is therefore normally seen in the chromatin of the XY bivalent (Ichijima et al. 2011). As observed for γH2AFX

(Fig. 2B), MDC1 localization to the XY chromatin was disrupted in the absence of ATR (Fig. 4A). We subsequently analyzed MDC1 and ATR localization in *H2AFX*$^{-/-}$ males (Fernandez-Capetillo et al. 2003). We observed defective spreading of both silencing proteins into the XY chromatin in this mutant (Fig. 4B). ATR localization to the XY axes was unaffected in *H2AFX*$^{-/-}$ males (Fig. 4B) as in *MDC1*$^{-/-}$ males (Ichijima et al. 2011), showing that neither MDC1 nor H2AFX is required for the sensing of unsynapsed chromosomes. We conclude that the effector step of meiotic silencing requires interdependence between ATR, MDC1, and H2AFX.

Finally we examined the effect of ATR loss on the localization of two other epigenetic modifications—SUMO-1 (Fig. 4C; Vigodner and Morris 2005) and ubiquitinated H2A (Fig. 4C; Baarends et al. 1999)—to the XY bivalent. SUMO-1 accumulation has been proposed to precede H2AFX phosphorylation on the sex chromosomes (Vigodner 2009; see also Ichijima et al. 2011), and H2A ubiquitination by the ligase UBR2 is thought to function independently of BRCA1/ATR in MSCI (An et al. 2010). In contrast to *Atr*$^{flox/+}$ males, in *Atr*$^{flox/-}$ males, we did not observe enrichment of either mark at the XY bivalent during pachytene. We conclude that acquisition of both SUMO-1 and ubiquitinated H2A on unsynapsed chromosomes is ATR-dependent.

Atr is dispensable for the maintenance of meiotic silencing

In *Atr*$^{flox/-}$ males, defective H2AFX phosphorylation on the XY bivalent was a highly penetrant phenotype, affecting all early pachytene cells in testis sections and giving rise to germ cell apoptosis at stages III and IV (Fig. 1A). However, ATR localization and H2AFX phosphorylation were grossly normal during late pachytene (Fig. 1D), and germ cells from stage VII onward appeared healthy (Fig. 1A), indicating that these later cells had evaded Cre-recombinase-mediated excision. Thus, *Atr*$^{flox/-}$ males could not be used to address the role of ATR in late meiosis.

To overcome this problem, we implemented a novel meiosis-specific gene knockdown strategy that uses MSCI to silence transcription of a chosen gene in a temporally precise manner (Fig. 5A). In this approach, a bacterial artificial chromosome (BAC) containing the *Atr* gene was targeted to the X chromosome. This was achieved by homologous recombination in mouse XY embryonic stem (ES) cells carrying BAC acceptor sites within the *Hprt1* locus (Prosser et al. 2008). Male "X^{Atr}Y" mice derived from these ES cells were then crossed onto an *Atr*-null background, generating complemented X^{Atr}Y$^{-/-}$ males whose only source of *Atr* originated from the X-inserted BAC. Expression of *Atr* from the X chromosome in X^{Atr}Y$^{-/-}$ embryos rescues the embryonic lethality; however, as meiotic cells undergo MSCI, the X-inserted copy of *Atr* is silenced, the result being that pachytene cells are *Atr*-null (Fig. 5A).

We generated complemented X^{Atr}Y$^{-/-}$ males from four independently targeted ES cell clones, which gave equivalent results. In control *Atr*$^{+/-}$ males, *Atr* expression, assayed by RNA FISH, was observed throughout pachytene, but in X^{Atr}Y$^{-/-}$ males, the X-inserted copy of *Atr* was silenced in early pachytene cells and remained inactive thereafter (Fig. 5B). As a result, a dramatic reduction in the level of ATR protein could be detected in X^{Atr}Y$^{-/-}$ relative to XY *Atr*$^{+/-}$ testes by Western blotting (Fig. 5C). We noted that in wild-type males, the majority

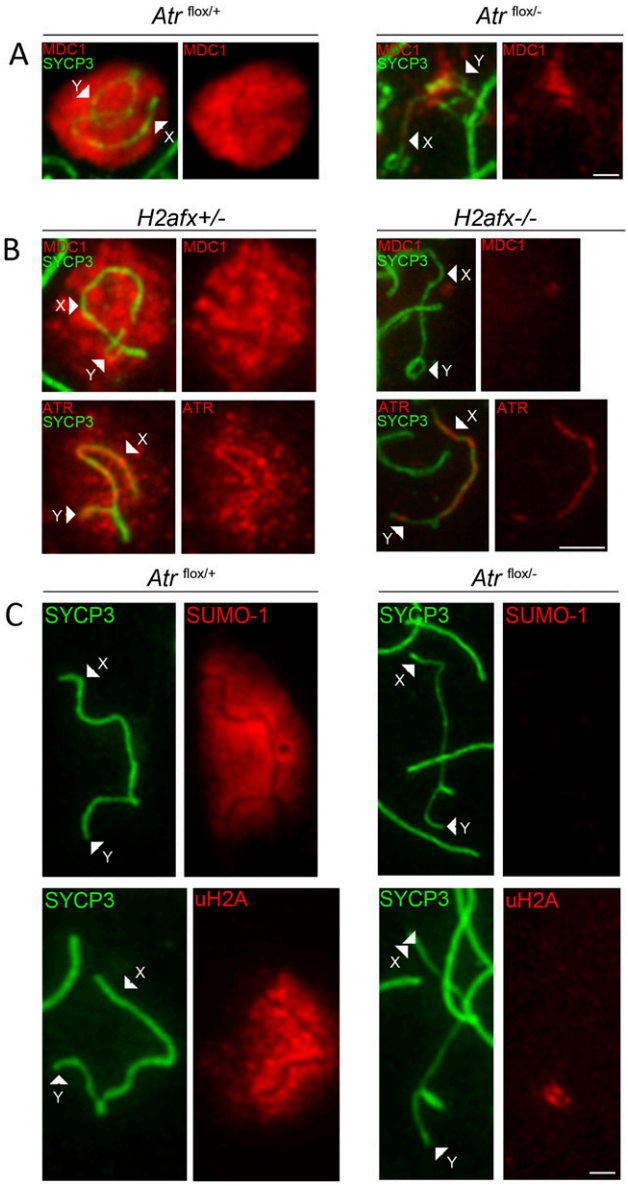

Figure 4. ATR, MDC1, and H2AFX phosphorylation are interdependent in the meiotic silencing pathway. (*A*) XY AEs from *Atr*$^{flox/+}$ and *Atr*$^{flox/-}$ surface spread pachytene spermatocytes showing disrupted MDC1 localization in *Atr*$^{flox/-}$ males (n = 50 nuclei). (*B*) XY AEs from surface spread control *H2afx*$^{+/-}$ and *H2afx*$^{-/-}$ pachytene spermatocytes showing disrupted MDC1 (*top* row,; n = 50 nuclei) and ATR (*bottom* row; n = 50 nuclei) localization in *H2afx*$^{-/-}$ males. (*C*) XY AEs from *Atr*$^{flox/+}$ and *Atr*$^{flox/-}$ surface spread pachytene spermatocytes showing disrupted SUMO-1 (*top* row; n = 50 nuclei) and ubiquitinated H2A (uH2A) (*bottom* row; n = 50 nuclei) localization in *Atr*$^{flox/-}$ males. Ubiquitinated H2A accumulates only at the PAR. (*A–C*) Arrowheads point to the X and Y AEs. Bar, 5 μm.

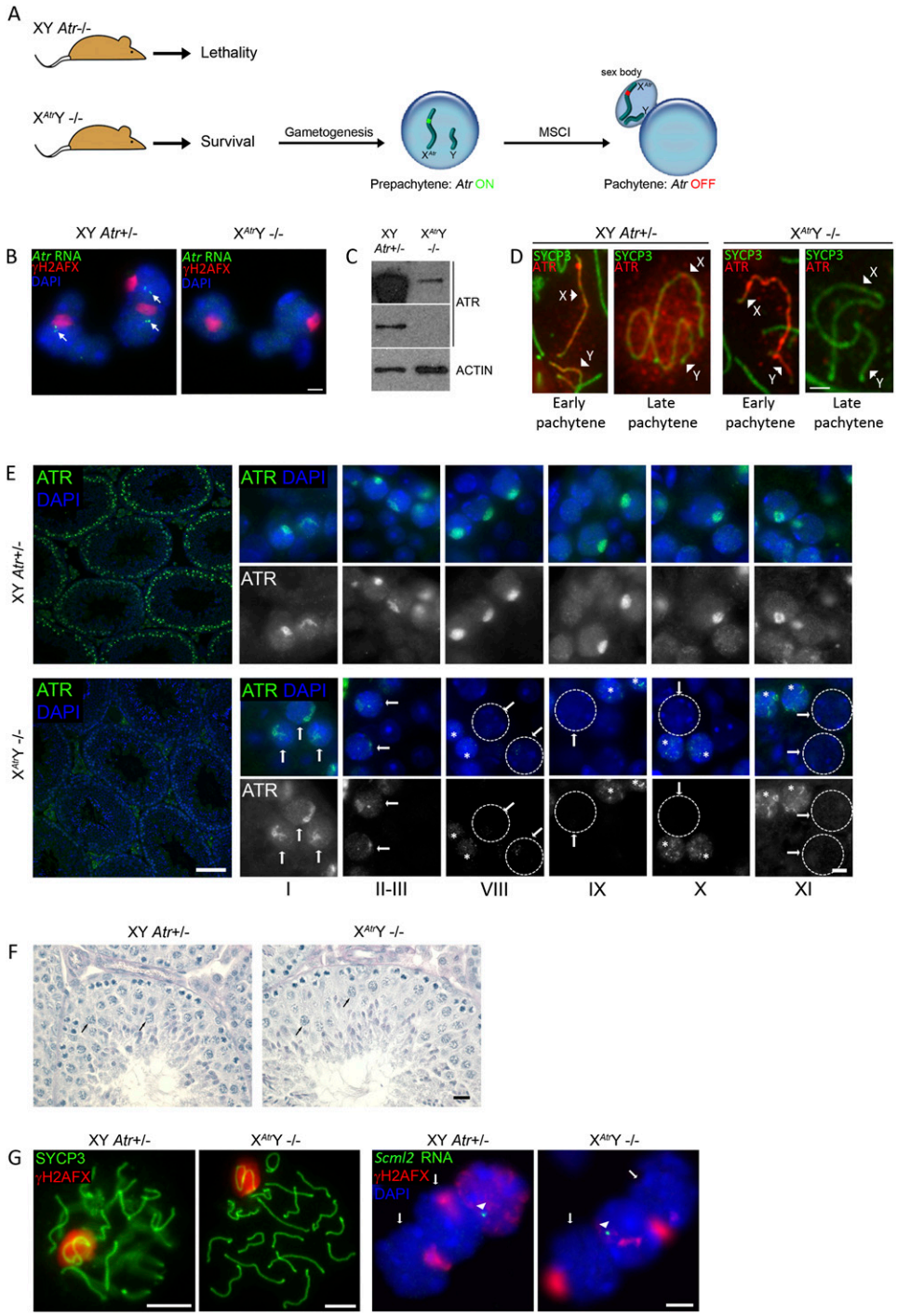

Figure 5. ATR is not required for the maintenance of meiotic silencing. (*A*) Cartoon showing the MSCI-mediated gene knockdown strategy. The *Atr* knockout lethality is overcome by an X-integrated *Atr* transgene in $X^{Atr}Y^{-/-}$ males. In germ cells, *Atr* is expressed from the transgene until it is shut down by MSCI at pachytene. (*B*) RNA FISH showing *Atr* expression (arrows) during pachytene in control XY $Atr^{+/-}$ (n = 100 nuclei) but not $X^{Atr}Y^{-/-}$ (n = 100 nuclei) males. Bar, 10 μm. (*C*) Western blot showing drastic reduction of ATR protein level in $X^{Atr}Y^{-/-}$ testis compared with XY $Atr^{+/-}$ testis. Two different exposure times are displayed for the ATR blot: Only with a long exposure time (shown at the *top*) is ATR detectable in $X^{Atr}Y^{-/-}$ testis. β-ACTIN is used as a loading control. (*D*) XY axes from XY $Atr^{+/-}$ and $X^{Atr}Y^{-/-}$ pachytene spermatocytes immunostained for ATR. ATR is present during early pachytene in both genotypes but is absent at late pachytene in $X^{Atr}Y^{-/-}$ males. Arrowheads point to the X and Y AEs. Bar, 5 μm. (*E*) Immunofluorescence of ATR on XY $Atr^{+/-}$ and $X^{Atr}Y^{-/-}$ testis sections. (*Left*) Low-magnification view of tubule sections showing drastic reduction of ATR signal in $X^{Atr}Y^{-/-}$ testis. (*Right*) At stage I, ATR is detected in the sex body and nucleoplasm of control and $X^{Atr}Y^{-/-}$ pachytene spermatocytes. In control pachytene cells, the same pattern persists until stage XI. In $X^{Atr}Y^{-/-}$ pachytene spermatocytes (arrows), the ATR signal is diminished even at stages II and III, and ATR is undetectable from stage VIII (ATR-depleted nuclei are delineated by dotted lines). Note that in stages VIII and XI, ATR is detected in $X^{Atr}Y^{-/-}$ prepachytene cells (asterisks), as expected. Bars: *left*, 100 μm; *right*, 5 μm. (*F*) PAS-stained stage IX tubule sections from $X^{Atr}Y^{-/-}$ and XY $Atr^{+/-}$ mice showing normal spermatogenesis. Arrows point to pachytene spermatocytes. Bars, 20 μm. (*G*, *left*) Surface spread image of pachytene control and $X^{Atr}Y^{-/-}$ cells showing normal H2AFX phosphorylation in the sex body of $X^{Atr}Y^{-/-}$ spermatocytes (n = 100 nuclei). (*Right*) RNA FISH image for control and $X^{Atr}Y^{-/-}$ pachytene cells (arrows). *Scml2* is silent at pachytene in both genotypes (n = 100 nuclei). Arrowheads point to *Scml2* RNA FISH signals in expressing prepachtyene cells. Arrows point to pachytene cells. Bars, 5 μm.

of ATR expression occurs during late pachytene (Fig. 1C). Since *Atr* silencing was observed at this stage in $X^{Atr}Y^{-/-}$ males (Fig. 5E) but not in $Atr^{flox/-}$ males (Fig. 1D), total ATR levels were lower in $X^{Atr}Y^{-/-}$ (Fig. 5C) than in $Atr^{flox/-}$ testes (Fig. 1B). Thus, MSCI can be used to silence gene expression during pachytene.

To establish when during spermatogenesis in $X^{Atr}Y^{-/-}$ males ATR protein levels were depleted, we analyzed ATR immunostaining in surface spreads. As expected, ATR was present on the XY chromatin at the point of initiation of MSCI but was undetectable during late pachytene (Fig. 5D). Subsequent immuno-analysis of $X^{Atr}Y^{-/-}$ testis sections confirmed normal ATR localization to the XY chromatin during MSCI initiation; i.e., at stage I of the seminiferous cycle (Fig. 5E). However, from stage II onward, the level of ATR on the XY bivalent was diminished, and no ATR staining could be observed by stage VIII (Fig. 5E). We conclude that, in wild-type males, ATR recruitment to unsynapsed chromatin is ongoing and dynamic and that *Atr* expression can be disrupted by MSCI-mediated knockdown.

Despite ablation of *Atr* expression, testis weights in $X^{Atr}Y^{-/-}$ males (mean 93 ± 14 mg, n = 4 males) were similar to those of XY $Atr^{+/-}$ control siblings (mean 91 ± 10 mg, n = 9 males), and $X^{Atr}Y^{-/-}$ males were fertile, with grossly normal testis histology (Fig. 5F). Moreover, XY H2AFX phosphorylation and MSCI, assayed by *Scml2* RNA FISH, were established and maintained normally in $X^{Atr}Y^{-/-}$ males (Fig. 5G). Interestingly, silencing factors (e.g., BRCA1, $HORMAD1^{Ser375}$, and $HORMAD2^{Ser271}$) localized normally at the XY AEs in late pachytene $X^{Atr}Y^{-/-}$ cells (Supplemental Fig. 1E) despite the absence of ATR at this stage (Fig. 5D,E). We observed no localization of ATM to the XY chromatin in late pachytene $X^{Atr}Y^{-/-}$ cells, suggesting that this kinase does not maintain H2AFX phosphorylation in the absence of ATR (Supplemental Fig. 1F). We conclude that ATR is dispensable for the maintenance of H2AFX phosphorylation and XY silencing and that, once established early in pachytene, meiotic silencing is remarkably stable.

Discussion

Here we demonstrate a role for ATR in the initiation of meiotic silencing. Our data show that *Atr* ablation cannot be compensated for by *Atm* and *DNA-PK* and are consistent with ATR being the major kinase that phosphorylates H2AFX to initiate XY inactivation. In addition, we show that ATR functions earlier in meiotic silencing by operating in conjunction with BRCA1, ATRIP, and TOPBP1 and regulating HORMAD1/2 phosphorylation at unsynapsed axes.

A recurrent theme that emerges from our work is that meiotic silencing involves a complex interplay between ATR and other silencing effectors. This can be understood in the context of a model that integrates current and existing observations with the sequential steps in the silencing process (Fig. 6). Initial sensing of unsynapsed axes during zygotene is HORMAD1-, HORMAD2-, and BRCA1-dependent but ATR-independent (Fig. 6A). This is consistent with findings in $Spo11^{-/-}$ mice that show that HORMAD1, HORMAD2, and BRCA1 localize along unsynapsed axes during zygotene independently of ATR accumulation (Mahadevaiah et al. 2008; Wojtasz et al. 2009). Subsequently, ATR is recruited to sites of asynapsis in a HORMAD1-, HORMAD2-, and BRCA1-dependent manner (Fig. 6B). Once recruited, ATR–ATRIP then facilitates further enrichment of BRCA1 as well as other factors involved in ATR activation; e.g., TOPBP1 and phosphorylation of HORMAD1/2. These events maintain asynapsis signaling at chromosome axes during late zygotene (Fig. 6C). Our data (Fig. 3) show that this ATR-dependent phase of silencing factor recruitment is dynamic. This flexibility may ensure that silencing factors can be rapidly evicted from AEs should homologs eventually achieve synapsis. However, if asynapsis persists at

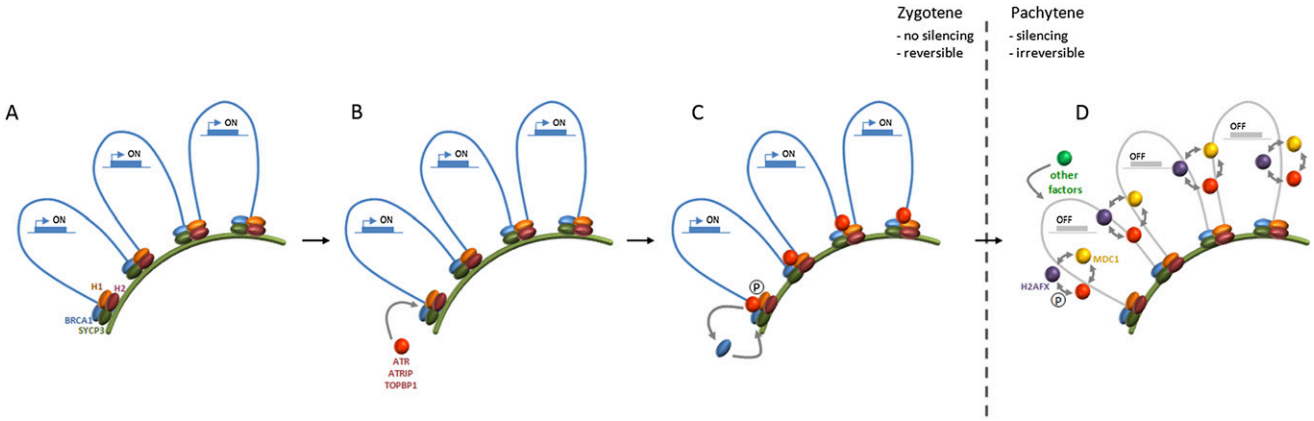

Figure 6. Model explaining the stage-specific requirements of ATR in meiotic silencing. (*A*) During zygotene, HORMAD1, HORMAD2, and BRCA1 associate with SYCP3-positive unsynapsed AEs independently of ATR. (*B*) This sensing complex is essential for subsequent ATR, ATRIP, and TOPBP1 recruitment at these sites. (*C*) ATR then facilitates ongoing asynapsis signaling through continued BRCA1 recruitment. (*D*) At the onset of pachytene, ATR translocates into chromatin loops, catalyzing H2AFX phosphorylation in a positive feedback loop with H2AFX and MDC1, resulting in recruitment of other silencing factors (e.g., ubiquitinated H2A) and irreversible gene silencing.

early pachytene, ATR subsequently translocates into chromatin loops of unsynapsed regions, leading to induction of repressive post-translational modifications (e.g., γH2AFX) and irreversible gene silencing over many megabases (Fig. 6D). Thus, ATR can be viewed as an adaptor protein, linking the sensor and effector arms of the silencing response. Once established, repressive chromatin marks do not require continued ATR activity for their maintenance. Likewise, at this stage, the maintenance of silencing factors at unsynapsed AEs also becomes ATR-independent (Fig. 6D).

In this study, we also present a novel genetic strategy whereby the expression of a gene of interest can be silenced in the germline using MSCI. We used this to demonstrate that loss of ATR after the initiation of XY inactivation does not impair H2AFX phosphorylation or the maintenance of silencing. Our data suggest that H2AFX phosphorylation is not an ongoing process but is restricted to early in pachytene, a property that contrasts with the more dynamic behavior of other histone modifications (e.g., H3K9me3) during the maintenance phase of MSCI (van der Heijden et al. 2007). Notably, the X-targeting strategy described here leads to dramatic and sustained depletion of gene expression. It may therefore prove superior to Cre recombinase-based approaches, which exhibit mosaic Cre-expression and varying excision efficiencies, in interrogating the functions of genes expressed during late prophase or spermiogenesis.

Curiously, the residual ATR protein that we observed in early pachytene $Atr^{flox/-}$ cells localized to the PAR. This finding is surprising because synapsed regions are normally devoid of ATR staining and because ATR was not observed on other synapsed bivalents in this model (Fig. 1D). Although currently difficult to reconcile, this abnormal localization may hint at defects in synapsis and/or recombination in $Atr^{flox/-}$ meiosis that are more pronounced at the PAR. The PAR exhibits unusual properties in meiosis, including delayed DNA DSB formation and synapsis (Kauppi et al. 2011). Work in other organisms has shown that ATR does indeed regulate synapsis and recombination as well as other fundamental aspects of meiosis, including interhomolog bias, crossover formation, and checkpoint responses (Carballo and Cha 2007). Although dispensable for the maintenance of H2AFX phosphorylation, the persistent ATR observed on unsynapsed chromosomes may be related to one or more of these processes. The application of the conditional approaches for ablating *Atr* described here will provide a unique opportunity to examine whether these functions are conserved in mammals.

Materials and methods

Mice

H2afx$^{-/-}$ (Fernandez-Capetillo et al. 2003) and *Atm*$^{-/-}$ (Barlow et al. 1996) mice were maintained on an MF1 background and according to United Kingdom Home Office regulations. $Atr^{flox/-}$ Cre-ERT2 males were as described (Ruzankina et al. 2007). Targeting of the *Atr* BAC into the X-linked *Hprt* locus by recombination-mediated cassette exchange in ES cells was performed as described previously (Prosser et al. 2008). All mice used in this project were maintained according to United Kingdom Home Office regulations.

Tamoxifen treatment

$Atr^{flox/-}$ Cre-ERT2 males were treated with tamoxifen at doses already described (Ruzankina et al. 2007). Males culled immediately after treatment cessation did not exhibit meiotic phenotypes, while those culled 3 d after treatment cessation showed mid-pachytene arrest. This implies that ATR excision occurred during an early, premeiotic germ cell type some 7–10 d prior to mid-pachytene. This is most likely to be a late stage A spermatogonial or early intermediate spermatogonial stage. We noted that as early as 1 mo after treatment cessation, $Atr^{flox/-}$ Cre-ERT2 males exhibited agametic tubules resulting from spermatogonial stem cell depletion. This is consistent with previous findings (Ruzankina et al. 2007) and meant that $Atr^{flox/-}$ Cre-ERT2 males cannot regain fertility after tamoxifen treatment.

RNA FISH, immunofluorescence, and Western blotting

Scml2 RNA FISH was carried out with digoxigenin-labeled probes as described (Mahadevaiah et al. 2009) using BAC RP24-204O18 (CHORI). Immunofluorescence experiments on surface spread spermatocytes were carried out as described in Turner et al. (2005) with antibody dilutions for SYCP3, BRCA1, ATR, and BRCA1 described in Turner et al. (2004); HORMAD1, HORMAD2, and TOPBP1 (gift from J. Chen) described in Wojtasz et al. (2009); and Ser375-phosphorylated HORMAD1 described in Fukuda et al. (2012). The ATRIP antibody (gift from K. Cimprich), MDC1 antibody (ABDSerotec), and SUMO-1 antibody (Abcam; ab11672) were used at 1:100. ATM antibodies pS1981-ATM (Rockland), 07-1286 (Miilipore), and H-248 (Santa Cruz Biotechnology) were used at 1:50. The Ser271-phosphorylated HORMAD2 antibody was made using the peptide EEEACG-S(PO3H2)-QVQRMN to immunize two rabbits. The same peptide was used to affinity-purify antibodies from the serum of immunized rabbits. EEEACGSQVQRMN peptide-coupled affinity resin was used to deplete antibodies that recognize the nonphosphorylated form of the immunizing peptide. Testis section immunofluorescence and Western blots (with ATR and β-ACTIN antibodies used at 1:1000 and 1:50 000, respectively) were carried out as described in Hamer et al. (2004). HORMAD1 and HORMAD2 quantitation was performed as described in Mahadevaiah et al. (2008).

Microscopy

For imaging, an Olympus IX70 inverted microscope with a 100-W mercury arc lamp using a 100× 1.35 U-PLAN-APO oil immersion objective (Olympus) or a 40× objective was used. Images were captured using a computer-assisted (Deltavision), liquid-cooled CCD camera (photometrics CH350L; sensor: Kodak KAF1400, 1317 × 1035 pixels). Each channel was captured separately as a 12-bit source image, and captured images were processed using ImageJ 1.46a.

Acknowledgments

We thank Karlene Cimprich and Junjie Chen for providing the ATRIP and TOPBP1 antibodies, respectively; Grzegorz Polikiewicz for genotyping; and Paul Burgoyne and members of Turner laboratory for critical reading of the manuscript. This work was funded by the Medical Research Council (U117588498), the

National Institute on Aging (2R01AG027376), the Deutsche Forschungsgemeinschaft (TO 421/3-1, 421/3-2, 421/4-1, and 421/5-1), the Wellcome Trust (WT098051), the Swedish Cancer Society, the Swedish Research Council, and the Karolinska Institutet.

References

An JY, Kim EA, Jiang Y, Zakrzewska A, Kim DE, Lee MJ, Mook-Jung I, Zhang Y, Kwon YT. 2010. UBR2 mediates transcriptional silencing during spermatogenesis via histone ubiquitination. *Proc Natl Acad Sci* **107:** 1912–1917.

Baarends WM, Hoogerbrugge JW, Roest HP, Ooms M, Vreeburg J, Hoeijmakers JH, Grootegoed JA. 1999. Histone ubiquitination and chromatin remodeling in mouse spermatogenesis. *Dev Biol* **207:** 322–333.

Baarends WM, Wassenaar E, van der Laan R, Hoogerbrugge J, Sleddens-Linkels E, Hoeijmakers JH, de Boer P, Grootegoed JA. 2005. Silencing of unpaired chromatin and histone H2A ubiquitination in mammalian meiosis. *Mol Cell Biol* **25:** 1041–1053.

Barlow C, Hirotsune S, Paylor R, Liyanage M, Eckhaus M, Collins F, Shiloh Y, Crawley JN, Ried T, Tagle D, et al. 1996. Atm-deficient mice: A paradigm of ataxia telangiectasia. *Cell* **86:** 159–171.

Bellani MA, Romanienko PJ, Cairatti DA, Camerini-Otero RD. 2005. SPO11 is required for sex-body formation, and Spo11 heterozygosity rescues the prophase arrest of $Atm^{-/-}$ spermatocytes. *J Cell Sci* **118:** 3233–3245.

Brown EJ, Baltimore D. 2000. ATR disruption leads to chromosomal fragmentation and early embryonic lethality. *Genes Dev* **14:** 397–402.

Burgoyne PS, Mahadevaiah SK, Turner JM. 2009. The consequences of asynapsis for mammalian meiosis. *Nat Rev Genet* **10:** 207–216.

Burrows AE, Elledge SJ. 2008. How ATR turns on: TopBP1 goes on ATRIP with ATR. *Genes Dev* **22:** 1416–1421.

Carballo JA, Cha RS. 2007. Meiotic roles of Mec1, a budding yeast homolog of mammalian ATR/ATM. *Chromosome Res* **15:** 539–550.

Carballo JA, Johnson AL, Sedgwick SG, Cha RS. 2008. Phosphorylation of the axial element protein Hop1 by Mec1/Tel1 ensures meiotic interhomolog recombination. *Cell* **132:** 758–770.

Daniel K, Lange J, Hached K, Fu J, Anastassiadis K, Roig I, Cooke HJ, Stewart AF, Wassmann K, Jasin M, et al. 2011. Meiotic homologue alignment and its quality surveillance are controlled by mouse HORMAD1. *Nat Cell Biol* **13:** 599–610.

Fernandez-Capetillo O, Mahadevaiah SK, Celeste A, Romanienko PJ, Camerini-Otero RD, Bonner WM, Manova K, Burgoyne P, Nussenzweig A. 2003. H2AX is required for chromatin remodeling and inactivation of sex chromosomes in male mouse meiosis. *Dev Cell* **4:** 497–508.

Fukuda T, Pratto F, Schimenti JC, Turner JM, Camerini-Otero RD, Hoog C. 2012. Phosphorylation of chromosome core components may serve as axis marks for the status of chromosomal events during mammalian meiosis. *PLoS Genet* **8:** e1002485.

Greaves IK, Rangasamy D, Devoy M, Marshall Graves JA, Tremethick DJ. 2006. The X and Y chromosomes assemble into H2A.Z-containing facultative heterochromatin following meiosis. *Mol Cell Biol* **26:** 5394–5405.

Hamer G, Kal HB, Westphal CH, Ashley T, de Rooij DG. 2004. Ataxia telangiectasia mutated expression and activation in the testis. *Biol Reprod* **70:** 1206–1212.

Handel MA, Schimenti JC. 2010. Genetics of mammalian meiosis: Regulation, dynamics and impact on fertility. *Nat Rev Genet* **11:** 124–136.

Ichijima Y, Ichijima M, Lou Z, Nussenzweig A, Camerini-Otero RD, Chen J, Andreassen PR, Namekawa SH. 2011. MDC1 directs chromosome-wide silencing of the sex chromosomes in male germ cells. *Genes Dev* **25:** 959–971.

Ichijima Y, Sin HS, Namekawa SH. 2012. Sex chromosome inactivation in germ cells: Emerging roles of DNA damage response pathways. *Cell Mol Life Sci* **69:** 2559–2572.

Inagaki A, Schoenmakers S, Baarends WM. 2010. DNA double strand break repair, chromosome synapsis and transcriptional silencing in meiosis. *Epigenetics* **5:** 255–266.

Kauppi L, Barchi M, Baudat F, Romanienko PJ, Keeney S, Jasin M. 2011. Distinct properties of the XY pseudoautosomal region crucial for male meiosis. *Science* **331:** 916–920.

Kouznetsova A, Wang H, Bellani M, Camerini-Otero RD, Jessberger R, Hoog C. 2009. BRCA1-mediated chromatin silencing is limited to oocytes with a small number of asynapsed chromosomes. *J Cell Sci* **122:** 2446–2452.

Lou Z, Minter-Dykhouse K, Franco S, Gostissa M, Rivera MA, Celeste A, Manis JP, van Deursen J, Nussenzweig A, Paull TT, et al. 2006. MDC1 maintains genomic stability by participating in the amplification of ATM-dependent DNA damage signals. *Mol Cell* **21:** 187–200.

Mahadevaiah SK, Bourc'his D, de Rooij DG, Bestor TH, Turner JM, Burgoyne PS. 2008. Extensive meiotic asynapsis in mice antagonises meiotic silencing of unsynapsed chromatin and consequently disrupts meiotic sex chromosome inactivation. *J Cell Biol* **182:** 263–276.

Mahadevaiah SK, Costa Y, Turner JM. 2009. Using RNA FISH to study gene expression during mammalian meiosis. *Methods Mol Biol* **558:** 433–444.

McKee BD, Handel MA. 1993. Sex chromosomes, recombination, and chromatin conformation. *Chromosoma* **102:** 71–80.

Modzelewski AJ, Holmes RJ, Hilz S, Grimson A, Cohen PE. 2012. AGO4 regulates entry into meiosis and influences silencing of sex chromosomes in the male mouse germline. *Dev Cell* **23:** 251–264.

Nagaoka SI, Hassold TJ, Hunt PA. 2012. Human aneuploidy: Mechanisms and new insights into an age-old problem. *Nat Rev Genet* **13:** 493–504.

Namekawa SH, Park PJ, Zhang LF, Shima JE, McCarrey JR, Griswold MD, Lee JT. 2006. Postmeiotic sex chromatin in the male germline of mice. *Curr Biol* **16:** 660–667.

Prosser HM, Rzadzinska AK, Steel KP, Bradley A. 2008. Mosaic complementation demonstrates a regulatory role for myosin VIIa in actin dynamics of stereocilia. *Mol Cell Biol* **28:** 1702–1712.

Refolio E, Cavero S, Marcon E, Freire R, San-Segundo PA. 2011. The Ddc2/ATRIP checkpoint protein monitors meiotic recombination intermediates. *J Cell Sci* **124:** 2488–2500.

Royo H, Polikiewicz G, Mahadevaiah SK, Prosser H, Mitchell M, Bradley A, de Rooij DG, Burgoyne PS, Turner JM. 2010. Evidence that meiotic sex chromosome inactivation is essential for male fertility. *Curr Biol* **20:** 2117–2123.

Ruzankina Y, Pinzon-Guzman C, Asare A, Ong T, Pontano L, Cotsarelis G, Zediak VP, Velez M, Bhandoola A, Brown EJ. 2007. Deletion of the developmentally essential gene ATR in adult mice leads to age-related phenotypes and stem cell loss. *Cell Stem Cell* **1:** 113–126.

Sedelnikova OA, Pilch DR, Redon C, Bonner WM. 2003. Histone H2AX in DNA damage and repair. *Cancer Biol Ther* **2:** 233–235.

Solari AJ. 1974. The behavior of the XY pair in mammals. *Int Rev Cytol* **38:** 273–317.

Song R, Ro S, Michaels JD, Park C, McCarrey JR, Yan W. 2009. Many X-linked microRNAs escape meiotic sex chromosome inactivation. *Nat Genet* **41:** 488–493.

Stiff T, O'Driscoll M, Rief N, Iwabuchi K, Lobrich M, Jeggo PA. 2004. ATM and DNA-PK function redundantly to phosphorylate H2AX after exposure to ionizing radiation. *Cancer Res* **64:** 2390–2396.

Turner JM, Aprelikova O, Xu X, Wang R, Kim S, Chandramouli GV, Barrett JC, Burgoyne PS, Deng CX. 2004. BRCA1, histone H2AX phosphorylation, and male meiotic sex chromosome inactivation. *Curr Biol* **14:** 2135–2142.

Turner JM, Mahadevaiah SK, Fernandez-Capetillo O, Nussenzweig A, Xu X, Deng CX, Burgoyne PS. 2005. Silencing of unsynapsed meiotic chromosomes in the mouse. *Nat Genet* **37:** 41–47.

Turner JM, Mahadevaiah SK, Ellis PJ, Mitchell MJ, Burgoyne PS. 2006. Pachytene asynapsis drives meiotic sex chromosome inactivation and leads to substantial postmeiotic repression in spermatids. *Dev Cell* **10:** 521–529.

van der Heijden GW, Derijck AA, Posfai E, Giele M, Pelczar P, Ramos L, Wansink DG, van der Vlag J, Peters AH, de Boer P. 2007. Chromosome-wide nucleosome replacement and H3.3 incorporation during mammalian meiotic sex chromosome inactivation. *Nat Genet* **39:** 251–258.

Vigodner M. 2009. Sumoylation precedes accumulation of phosphorylated H2AX on sex chromosomes during their meiotic inactivation. *Chromosome Res* **17:** 37–45.

Vigodner M, Morris PL. 2005. Testicular expression of small ubiquitin-related modifier-1 (SUMO-1) supports multiple roles in spermatogenesis: Silencing of sex chromosomes in spermatocytes, spermatid microtubule nucleation, and nuclear reshaping. *Dev Biol* **282:** 480–492.

Wojtasz L, Daniel K, Roig I, Bolcun-Filas E, Xu H, Boonsanay V, Eckmann CR, Cooke HJ, Jasin M, Keeney S, et al. 2009. Mouse HORMAD1 and HORMAD2, two conserved meiotic chromosomal proteins, are depleted from synapsed chromosome axes with the help of TRIP13 AAA-ATPase. *PLoS Genet* **5:** e1000702.

Wojtasz L, Cloutier JM, Baumann M, Daniel K, Varga J, Fu J, Anastassiadis K, Stewart AF, Remenyi A, Turner JM, et al. 2012. Meiotic DNA double-strand breaks and chromosome asynapsis in mice are monitored by distinct HORMAD2-independent and -dependent mechanisms. *Genes Dev* **26:** 958–973.

Yan W, McCarrey JR. 2009. Sex chromosome inactivation in the male. *Epigenetics* **4:** 452–456.